Optimization of spray-dried hyaluronic acid microspheres to formulate drug-loaded bone substitute materials

Mohamed Fatnassi [a], Sylvaine Jacquart [a], Fabien Brouillet [b], Christian Rey [a], Christèle Combes [a], Sophie Girod Fullana [b,*]

[a] Université Toulouse, CIRIMAT INPT-CNRS-UPS, ENSIACET, 31030 Toulouse, France
[b] Université Toulouse, CIRIMAT INPT-CNRS-UPS, Fac. Sciences Pharmaceutiques, 31062 Toulouse, France

Keywords:
Microspheres
Spray-drying
Hyaluronic acid
Controlled release
Bone cement

A B S T R A C T

We present here our first results concerning the evaluation of hyaluronic acid (HA) as a candidate to formulate an organic–mineral cement with sustained release properties. Incorporating drug-loaded microspheres in mineral bone cements is an alternative strategy to improve their ability as drug delivery materials. To synthesize microspheres according to a reproducible process and control at the same time their morphology and their encapsulation efficiency is one of the main challenges of the conception of such drug-loaded bone substitute. In this context, we investigated the potentialities of two HA, differing by their molecular weight, to form microspheres by a spray-drying technique. Erythrosin B (EB) was encapsulated as a model drug and spray-drying process conditions were optimized. To perform this, the rheological behavior and viscosity of HA solutions have been related to their spray-drying ability, and then to the resulting microparticles morphological properties and size distribution. Reproducible microspheres, answering to the requirements in terms of size and encapsulation efficiency, have been obtained from both HA. However the HA exhibiting the lowest molecular weight, HA600, led to smaller microparticles, with a higher polydispersity index. Their swelling ability, related to their stability upon rehydration, also appeared reduced. In this context, HA850, with the highest molecular weight, was selected and the possibility to modulate drug release by HA850 microspheres incorporation into a mineral cement was explored. EB release kinetics from HA microspheres, HA microspheres loaded cement and reference cement were followed at 37 °C, in Tris buffer at pH 7.4, using European Pharmacopoeia flow-through cells. Results showed that HA microspheres incorporation into a mineral cement permitted to modify the cement drug release profile and led to a sustained release.

1. Introduction

Hyaluronic acid (HA) is an abundant non-sulfated glycosaminoglycan component of synovial fluid and extracellular matrices. It is a mucopolysaccharide consisting of repeating units of D-glucuronic acid and N-acetyl-D-glucosamine (Fig. 1). It is a well-known biocompatible, nonimmunogenic and biodegradable polymer, having widespread applications in drug delivery, tissue engineering and viscosupplementation [1–6]. Besides being an important structural component in cartilage, HA is also essential for bone remodeling [7]. HA is an attractive starting material for the construction of bulk gels or hydrogel particles [8] but its applications in bone tissue engineering are limited by its poor mechanical properties. For this reason, it is often associated with calcium phosphates in order to obtain reinforced and/or injectable bone cements, consisting in HA gels containing hydroxyapatite [9,10] or calcium phosphate cements CPCs containing HA [11,12].

To minimize the risk of post-operative failure, surgeons often require the possibility to co-administer therapeutic agents and/or biologically active components limiting inflammation, bacteria proliferation or promoting bone reconstruction (antibiotics, growth factors…). In this context, CPCs can be used as local drug delivery systems [13,14]. An alternative approach for drug loading is to incorporate the drug in polymeric microspheres before blending with CPC. This strategy offers two advantages: polymer microparticles could help to modulate drug delivery [15–20], in combination with cohesion and/or enhanced resorption and remodelling capability [13,14].

Synthetic polymers, mainly poly(lactic-*co*-glycolic) acid PLGA, have been tested for this purpose [15,16,20], but their acidic degradation remains problematic. Surprisingly, polysaccharides have rarely been exploited to form microparticles [18] although they are frequently added to CPCs as rheological modifiers or cohesion promoters [21–23]. HA has never been tested for this purpose.

In this context, we decided to evaluate hyaluronic acid as a candidate to formulate a loaded microspheres–mineral cement whose release properties could be tailored on demand.

* Corresponding author.
E-mail address: sophie.fullana-girod@univ-tlse3.fr (S. Girod Fullana).

http://dx.doi.org/10.1016/j.powtec.2013.08.027

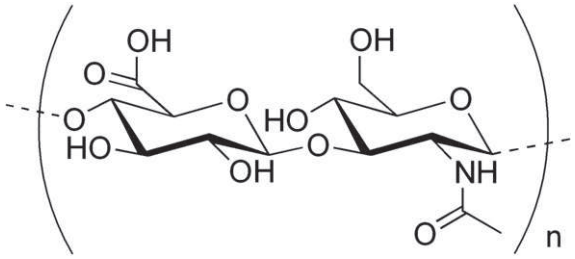

Fig. 1. Chemical structure of the monomer units of hyaluronic acid (HA).

To synthesize microspheres according to a reproducible process and control at the same time their morphology and their encapsulation efficiency is one of the main challenges of such organic–mineral cement design. Process conditions have to be optimized to fit the desired particles characteristics: (i) high encapsulation efficiency, (ii) spherical morphology, (iii) particles mean size and size distribution maintaining the injectability property of the final organic–mineral cement.

In this context, we explored the potentialities of two HA, differing by their molecular weight, to form microspheres with a spray-drying method. Spray-drying method consists of atomizing chemical solutions into droplets dispersed and dried inside a carrier gas, which induces a concentration of non-volatile species and the solidification of particles. It is extensively used in pharmaceutical industries [24,25], since the textural and release properties of the materials are highly tunable thanks to the variation of the solution components.

Erythrosin B (EB), a fluorescein derivative, was encapsulated as a model drug and spray-drying process conditions were optimized. To perform this, the rheological behavior and viscosity of HA solutions have been related to their spray drying ability, and then to the resulting microparticles morphological properties and size distribution. Then the release ability of a HA microspheres–mineral cement was evaluated and compared to the microspheres and the mineral cement release profiles.

2. Materials and methods

Two hyaluronic acid (HA) samples with high molecular weight were tested in this study. HA600 (Cristalhyal, Soliance, France, kindly provided by Pr R. Auzély-Velty from the CERMAV laboratory, Grenoble, France) and HA850 (Primalhyal, Soliance, France) exhibited an average molecular weight of 600,000 Da and 850,000 Da, respectively. Erythrosin B (Tetraiodofluorescein sodium salt, dye content 91.7%) was purchased from Alfa Aesar and Tris (Tris(hydroxymethyl)aminomethane Trizma® base BioXtra, purity ≥99.9%) from Sigma.

2.1. Preparation of HA and HA-EB solutions

Polymer solutions, with HA concentrations ranging from 1 g/L to 10 g/L, were obtained by dispersing polymer powder in deionized water under continuous stirring for 24 hours at room temperature.

2.2. Rheological characterization of HA in solution

Polymers rheological behavior, at concentrations ranging from 1 g/L to 10 g/L, was studied using a controlled stress rheometer (Haake Rheostress RS 75) equipped with a cone plate geometry (6 cm diameter; 1° angle). Measurements were obtained with imposed shear rate ranging from 0 to 2000 s^{-1}.

2.3. Production of HA microspheres: Spray-drying

Microparticles were produced using a Buchi mini Spray Dryer model 190 (Buchi, Germany). Briefly, the polymer solutions, with HA concentrations ranging from 1 g/L to 6 g/L, were fed into the instrument by a peristaltic pump and sprayed with a 0.7 mm nozzle, by means of a flow of compressed air, in the drying chamber of the apparatus. A flow of heated air aspirated by a pump induced the quick evaporation of the solvent from the drops, leading to the formation of solid microparticles. The instrumental settings are reported in Table 1. The obtained particles, after separation from the exhausted air cyclone, settled into a bottom collector and were kept in sealed tubes at ambient temperature prior use.

2.4. Microparticles characterization

Morphology (shape and surface) of the dried microspheres was observed by scanning electron microscopy (SEM) using a LEO 435VP microscope after metallization by silver coating under vacuum by SPI Sputter coating unit.

Particles size distributions were measured using a laser particle sizer Mastersizer 2000 (Malvern, UK) based on a laser light scattering technique. Each sample was measured in triplicate. The volume weighted mean diameters, (D [4,3]) and mean $D(0.5)$, were used to describe the particles size. The polydispersity or span of size distributions was evaluated by calculation of samples polydispersity index $PI = [D(0.9) - D(0.1)]/D(0.5)$

2.4.1. Microparticles recovery: Yield

Microparticles recovery efficiencies were calculated as percentage of weight of the obtained microparticles, taking as reference the total amount of polymer (and EB if added) used for their preparation.

2.4.2. Drug content of microparticles: Encapsulation efficiency

The amount of encapsulated drug per milligram of dried microspheres was determined by visible spectroscopy (Spectrophotometer HP 8451A) at 528 nm (wavelength value corresponding to the λ_{max} of EB), after complete degradation (i.e. after 72 hours) of 100 mg of microspheres into Tris buffer 0.1 M solution at pH 7.4, under stirring at 100 rpm at room temperature. Encapsulation efficiency was calculated by the ratio between this EB amount to the EB amount initially incorporated in the polymer solution.

2.5. Preparation of reference and microspheres-loaded cements

The reference mineral cement (MC) paste was prepared by mixing the appropriate amount of liquid phase (deionized water) with a powder mixture of brushite (DCPD, $CaHPO_4$, $2H_2O$) and vaterite ($CaCO_3$), as previously published [26]. Powder and liquid phase were mixed using a liquid/solid weight ratio of 0.7. In the case of reference EB-cements (MC-EB), EB was added in the solid phase. In the case of microspheres-loaded cements (MC-HA-EB), the required amount of microspheres (10% w/w of the solid phase of the cement) was added to the reference paste after 1 minute of mixing, and mixed until visually homogeneous distribution of the microparticles within the paste was obtained. The pastes were then filled into silicone moulds, placed in sealed containers and let at 37 °C in a water saturated atmosphere for 48 hours, while setting and hardening.

Table 1
Spray drying conditions. Spray-drying parameters of the microspheres manufactured (HA or EB-loaded HA microspheres) for this study using a Büchi B-290 equipment.

Spray-dryer parameters	HA600	HA600-EB	HA850	HA850-EB
Atomizing gas flow rate (L/h)	357	357	357	357
Drying gas flow rate (L/h)	30	30	30	30
Feedstock flow rate (L/h)	0.34	0.34	0.34	0.34
Inlet temperature (°C)	120	120	120	120
Outlet temperature (°C)	55	59	57	65

2.6. Microspheres stability

Microspheres stability with time was evaluated by studying their swelling in Tris buffer at pH 7.4. Swelling was estimated by weighing microspheres at determined intervals of time after immersion into the buffer, according to the equation:

$$\text{Microspheres swelling at time } t\ (\%) = [(m_t - m_0)/m_0] \times 100$$

where m_t is microspheres weight at time t, and m_0 is microspheres weight before immersion in buffer.

The procedure to perform this was standardized: a precise amount of microspheres of approximately 100 mg was put in a filter between glass beads and immersed in 10 mL of Tris buffer. At determined intervals of time, the buffer was removed by filtration under vacuum (by using a vacuum pump during 20 seconds) and the drained filter weighed. Then the experiment was carried on by immersing again the microspheres in the same amount of fresh buffer, until microspheres destructuration and complete gel erosion. This experiment was done 3 times for each sample and results were expressed as mean ± standard deviation.

2.7. In vitro release kinetics

2.7.1. Drug release conditions

Erythrosin B release profiles were obtained with a flow-through cell system, USP Apparatus 4 (Sotax CE6, Sotax AG, Switzerland) with 22.6 mm cells and a piston pump (Sotax CY7, Sotax AG, Switzerland). In all experiments laminar flow (with a bed of 5 g of glass beads) was used. The in vitro release tests were carried out at 37 °C ± 0.5 °C under sink conditions according to European Pharmacopoeia guidelines [27]. About 100 mg of microspheres or a block of hardened cement of about 1.5 g were placed above the glass beads and covered with 3 g more. The dissolution medium, Tris buffer 0.1 M (pH 7.4), was pumped through the column at a flow rate of 10 mL/min. A closed system was used, recycling 500 mL of dissolution medium. Periodically, fractions of 5 mL were collected and the drug content was determined by visible spectroscopy at 528 nm (Spectrophotometer HP 8451A), according to a standard curve (EB concentrations ranging from 1 mg/L to 15 mg/L, coefficient of determination $r^2 = 0.9998$). Same volume of dissolution medium was replaced back after each sampling in order to maintain sink conditions. For every trial, a standard curve was prepared. The in vitro release studies were performed in triplicate. Results were expressed as mean ± standard deviation.

2.7.2. Drug release analysis

The experimental release data were then fitted to the following semi-empirical equations respectively describing (i) Higuchi model, which is adapted to solid drugs dispersed in solid granular matrices [28], (ii) Weibull model, which is adapted to heterogeneous systems [29], and dissolutive release mechanism from microspheres [30].

Within Higuchi model, the ratio $Q(t)/Q_0$ between the cumulative percentage of drug released at time t and at infinite time is:

$$Q(t)/Q_0 = K_H \cdot t^{1/2} + c \quad \text{(i)}$$

where K_H is the dissolution constant, coefficient calculated by plotting the linear forms of the Higuchi equation.

Within Weibull model, $Q(t)/Q_0$ is:

$$Q(t)/Q_0 = 1 - \exp\left[-\left(t - t_{lag}\right)^b / t_{scale}\right] \quad \text{(ii)}$$

where t_{lag} is the lag time before drug release takes place, t_{scale} is indicative of the timescale for the release process and b characterizes the shape of the release curve.

To put in evidence a dissolutive release mechanism, $Q(t)/Q_0$ is plotted according to the following equation:

$$Q(t)/Q_0 = K_{Diff} \cdot t^{0.432} + c' \quad \text{(iii)}$$

K_{Diff} and c' are coefficients calculated by plotting the linear forms of the equation.

The release data up to the plateau of released drug were used to produce theoretical release curves.

2.8. Statistical analysis

Results are expressed as mean ± standard deviation. Statistical comparison of the data was performed using the t-test for comparison between two groups or one-way ANOVA and post hoc Boferroni's test for comparison of more than two groups. A value of $p < 0.05$ was considered significant.

3. Results and discussion

Two hyaluronic acid samples HA600 and HA850, with different average molecular weight, have been compared in order to determine the best candidate to form microspheres to incorporate in a mineral cement. The aim was to obtain microspheres of about 5 to 30 μm to preserve cement injectability, with the best yield. For this purpose, a spray-drying method was chosen. Although the production of HA microspheres by spray-drying has already been reported in the literature [2,6,5], the operating conditions can vary and may affect particle size and morphology. The choice of the HA type is also far from negligible as its behavior in solution and its molecular weight will directly impact the spray-drying process conditions, hence, microspheres morphology and rehydration after drying. The presence of an active compound in solution may also have an influence as it could modify in an unpredictable manner the viscosity of the solution to spray-dry. Moreover, the physico-chemical characteristics of the drug, in particular its hydrophilic–lipophilic balance, play a crucial role on the encapsulation efficiency value. In this study, our aim was to be in an ideal case, with a model hydrophilic molecule able to diffuse freely out of the microspheres, reference cement and composite. We decided to work with a hydrophilic model molecule, erythrosine B (EB). EB is a red fluorescent dye which can be easily assayed by fluorescence or absorption in the visible range (λ_{max} = 526–528 nm); its chemical formula is presented in Fig. 2. At neutral pH it is positively charged, avoiding the possibility of ionic interaction of the drug with the mineral phase of the cement in the dissolution–precipitation process taking place during setting (resulting in Ca^{2+} ions chelation) and adsorption on the components of the mineral cement.

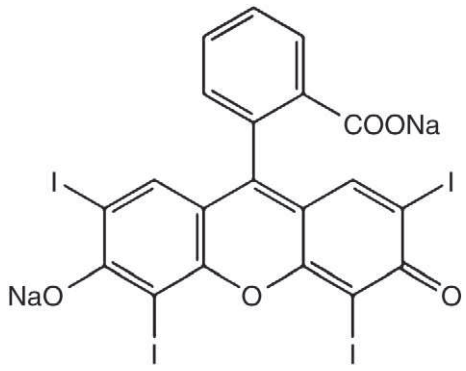

Fig. 2. Chemical structure of erythrosin B (EB).

3.1. Optimization of the operating conditions of the spray drying process

Various parameters may influence microspheres morphology and process yield. Some are directly correlated to the method: atomizing gas flow rate, drying gas flow rate, feedstock flow rate, and inlet temperature [24] (see Table 1 for the instrumental settings used in this study). Others depend on the properties of the solutions to spray-dry. To control this parameter, we decided to rely the rheological properties of the HA solutions to their ability to be spray-dried. HA solutions of concentrations ranging from 1 to 10 g/L have been characterized with a rheometer before being spray-dried. The resulting microspheres have been observed by SEM and their size distribution was determined. As an example the results obtained for HA600 are shown in Fig. 3.

All the HA solutions exhibited a shear-thinning behavior and were nonthixotropic. A concentration of 1 g/L appeared as the minimum threshold of concentration to obtain microspheres, and a concentration of 6 g/L resulted in too viscous solutions. Between these limits, HA concentration did not seem to influence the resulting microspheres morphology (Fig. 3). They look for the most part spherical, with a smooth surface. However, their size distribution appeared correlated to the viscosity of the initial HA solutions. Liu et al., who investigated the influence of polymer concentration on the size and morphology of spray-dried chitosan microparticles, led to the same observations [31]. In our case, increasing HA concentration increased particles sizes and spray-drying yield, by decreasing the rate of small particles, which are more difficult to collect and impact the polydispersity index (PI) of the batches. As a consequence, HA concentration, in the range from 1 to 4 g/L, had a significant effect on particle size, as demonstrated by statistical analysis ($p < 0.05$).

We explored the influence of HA type and EB presence on the rheology of HA solutions, and their consecutive spray-dry-ability. Concerning the influence of HA type, a comparison of the viscosities of HA600 and HA850 solutions at 1000 s^{-1} is shown in Fig. 4. As

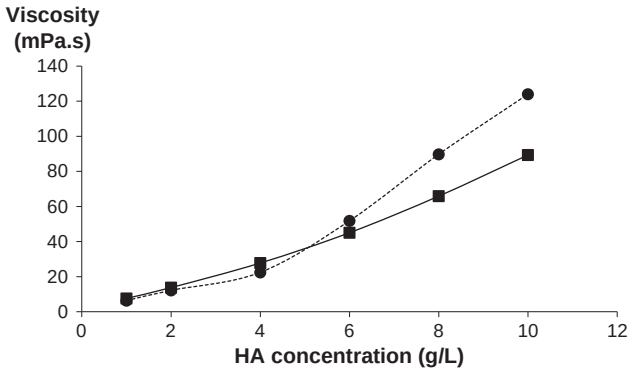

Fig. 4. Evolution of the viscosity of HA solutions at 1000 s^{-1} as a function of polymer concentration and average molecular weight (●, dotted line: HA600; ■, full line: HA850).

expected, increasing HA concentrations increased HA solutions viscosity. The HA850 viscosity appeared higher but close to the one of HA600 at low concentrations; however the phenomenon was reversed for concentrations higher than 5 g/L, perhaps due to smaller chains entanglement. The results obtained in terms of morphology and size distribution of the particles made us choose to work with concentrations of 4 g/L, just below the maximum threshold of concentration allowing spray-drying. These conditions permitted to obtain HA microspheres in a reproducible manner, with polydispersity indexes lower than 3 for both HA tested (Table 2). Using spray-drying to produce HA microspheres presents many advantages. In comparison with solvent evaporation after emulsification, a competitor method to produce microspheres, spray-drying results in a one-pot synthesis, avoiding time-consuming steps and the use of harsh solvents [32]. It is compatible

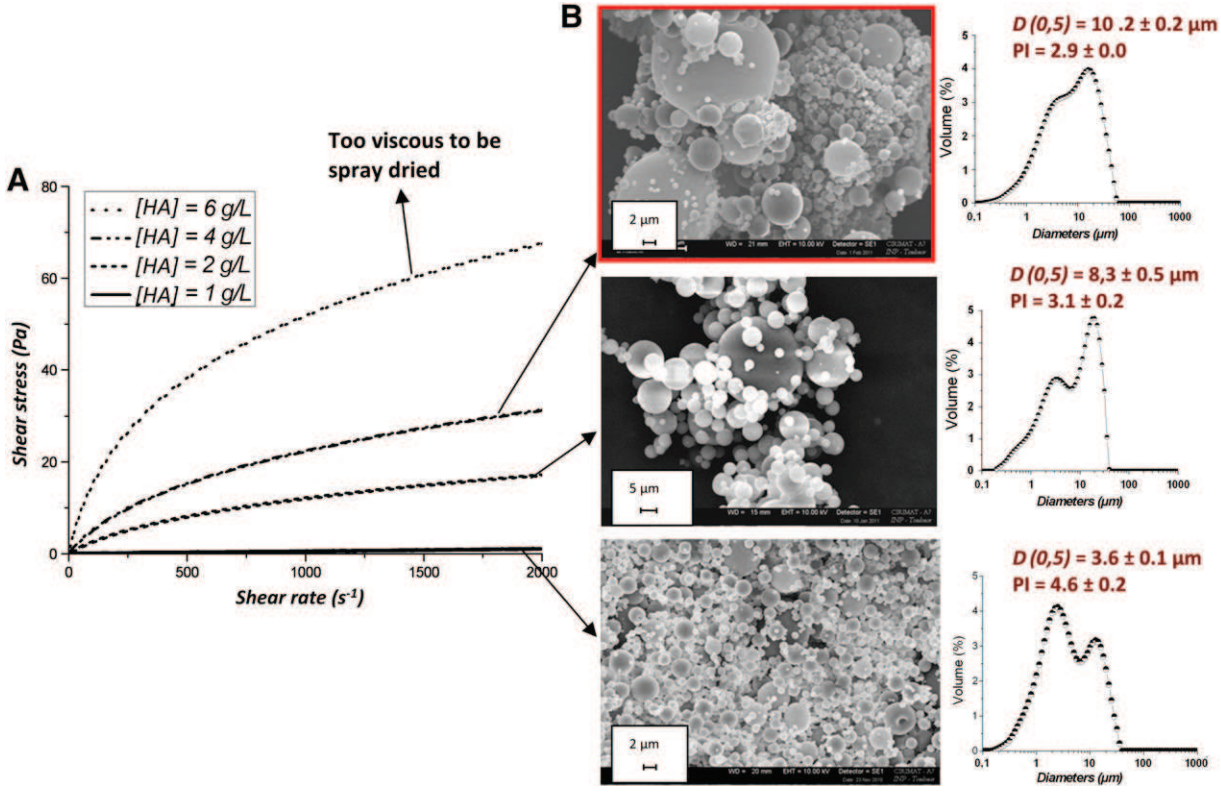

Fig. 3. Rheological behavior of HA600 in solution and resulting microspheres characteristics after spray-drying: A) flow curves of HA solutions at various concentrations; B) resulting microspheres morphological properties after spray-drying of the solutions: SEM micrographs and particle size distributions.

Table 2
Main characteristics of the HA solutions (composition, viscosity) and resulting HA microspheres after spray-drying experiments (yield, encapsulation efficiency, morphology and granulometry).

Samples	HA600	HA600-EB	HA850	HA850-EB
HA concentration (g/L)	4	4	4	4
EB/HA ratio (% w/w)	–	12.5	–	12.5
Viscosity (mPa s)[a]	22.4	20.9	27.8	18
Spray-drying conditions				
Yield (%)[b]	37	45	27	46
Encapsulation efficiency (%)[c]	–	89	–	93
Morphology	Spherical shape	Spherical shape	Spherical shape	Spherical shape
D (0.5) (μm)	10.2 ± 0.2	8.7 ± 0.1	28.8 ± 0.2	18.1 ± 0.7
D [4.3] (μm)	13.8 ± 0.3	12.8 ± 0.3	37.3 ± 2.9	25.8 ± 4.1
PI[d]	2.9 ± 0.0	3.3 ± 0.0	2.3 ± 0.1	2.8 ± 0.1

[a] Viscosity values for a shear rate of 1000 s^{-1}.
[b] Ratio between microspheres collected at the end of the spray-dryer cyclone and the initial quantity of nonvolatile matter (polysaccharide and EB) in solution.
[c] Determined by visible spectrometry at 528 nm.
[d] Polydispersity index corresponding to $(D(0.1) - D(0.9))/D(0.5)$.

with on-line continuous production and easily scaled up, a necessity for further industrial development.

Concerning the influence of EB on HA solutions, it resulted in a decrease of the viscosity at 1000 s^{-1} of 6 to 10 mPa s, whatever the HA molecular weight and the HA concentration tested. As an example, the viscosities measured for various concentrations of HA850, in presence or absence of EB in solution, are shown in Fig. 5. As this decrease of viscosity of HA solutions did not notably impact HA particles morphology, we kept the same HA concentration of 4 g/L as operating condition for the following HA-EB microspheres synthesis.

3.2. Microspheres characterization

Fig. 6 shows the morphology of the HA microparticles with or without drug obtained with the optimized conditions. Table 2 reports microspheres main characteristics (EB contents, encapsulation efficiencies and sizes).

High EB encapsulation efficiencies were obtained. In all cases, particles with a spherical morphology and a smooth surface were observed. Their D(0.5) ranging from 8.8 to 28.1 μm remained compatible with the injectability of the further polymer–mineral substitutes. However, HA molecular weight influence appeared significant on particle size: HA850 permitted to obtain microspheres with larger D(0.5) and D [4,3], lower polydispersity index (PI) ($p < 0.05$) and higher encapsulation efficiency.

Results were well correlated with the rheometric study, since HA600 solutions, less viscous, led to smaller particles with a higher polydispersity index ($p < 0.05$). Ré et al., who studied the influence

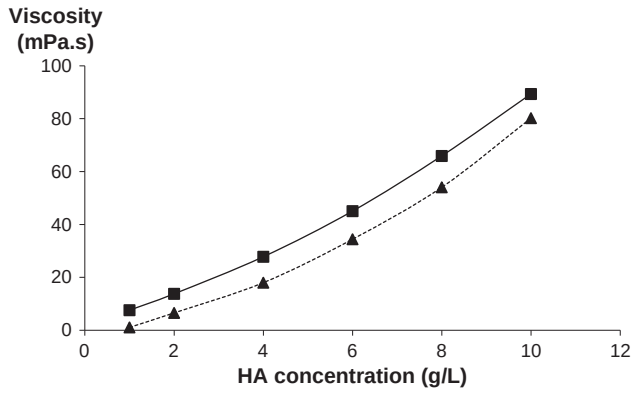

Fig. 5. Influence of EB addition on the viscosity of HA solutions at various concentrations (■, full line: H850; ▲, dotted line: HA850-EB).

of the liquid properties on the physical properties of spray-dried microparticles, reported similar observations: larger droplets were formed by increasing the liquid viscosity and surface tension [33]. Given that the presence of EB had a small influence on HA600 and HA850 solutions viscosity, it induced a slight decrease in particle sizes and an increase of PI when comparing solutions of the same polymer with or without EB.

Prior in vitro studies, the stability of HA600 and HA850 microspheres upon rehydration was explored by following their swelling with time after immersion in Tris buffer at pH 7.4 (Fig. 7). Both formulations presented the same rehydration profile, consisting in a rapid liquid absorption followed by a plateau and a progressive loss of weight due to microspheres disintegration. HA850 microspheres swelling was faster: they reached 2000% within the first 2 minutes, while HA600 microspheres reached 1200% after 3 hours. Progressively, HA microspheres became a loose gel before dissolving completely into the medium after 22 hours and 29 hours of immersion for HA600 and HA850 microspheres, respectively. HA850 microspheres higher resistance resulted from HA higher molecular weight. Regarding all the results, HA850 was selected to test its in vitro release abilities.

3.3. In vitro release of EB from HA850 microspheres (HA), microspheres loaded cements (MC-HA) and reference mineral cements (MC)

As an example, HA microspheres were incorporated in a mixed calcium carbonate–calcium phosphate cement (further called MC: mineral cement). In vitro release experiments were conducted on HA, MC-HA and MC materials at 37 °C, in Tris buffer at pH 7.4, using European Pharmacopoeia flow-through cells. Results are presented in Fig. 8. Microspheres, microspheres loaded and reference cements led to different release profiles. In the case of HA microspheres, EB release was fast: it reached 79% in 7.5 hours and was complete in a lag time of 30 hours. This result is in agreement with HA microspheres stability in solution (Fig. 7). Both materials (MC and MC-HA) exhibited sustained release profiles, which appeared superimposable on the first 7.5 hours, clearly showing that the mineral matrix and its porosity were the limiting factors of the release on the first hours. EB release at this time was 33.5% for MC-EB and 32.6% for MC-HA-EB. After 7.5 hours, the EB release from reference cement remained significantly higher than that of microspheres loaded cement, which appeared sustained. Only 57.7% of EB was released after 47 hours in the case of MC-HA-EB.

The shapes of the curves, combined with the mathematical analysis of the data, clearly show that the drug release modalities were complex, and different in the three cases. The resulting kinetic parameters estimated from Higuchi and Weibull models (see Material and methods) are presented in Table 3.

Table 3
Release kinetics parameters of EB release from HA850 microspheres (HA-EB), HA850 microspheres loaded cement (MC-HA-EB) and reference mineral cement (MC-EB).

Sample name	AH-EB	MC-HA-EB	MC-EB
Synthesis			
Ratio HA/solid phase (% w/w)	–	10	–
Ratio EB/solid phase (% w/w)	10	1	1
Release properties			
Higuchi model			
K_H dissolution constant ($h^{-1/2}$)	0.233	0.078	0.116
Coefficient of determination r^2	0.986	0.971	0.999
Weibull model			
Q_0	93	65	70
B	0.77	0.41	0.57
t_{lag} (hour)	0.088	0.14	0
t_{scale} (hour)	3.29	11.59	6.99
Coefficient of determination r^2	0.998	0.995	0.997
Dissolutive model			
K_{Diff}	−0.2049	−0.0193	−0.0324
Coefficient of determination r^2	0.998	0.891	0.982

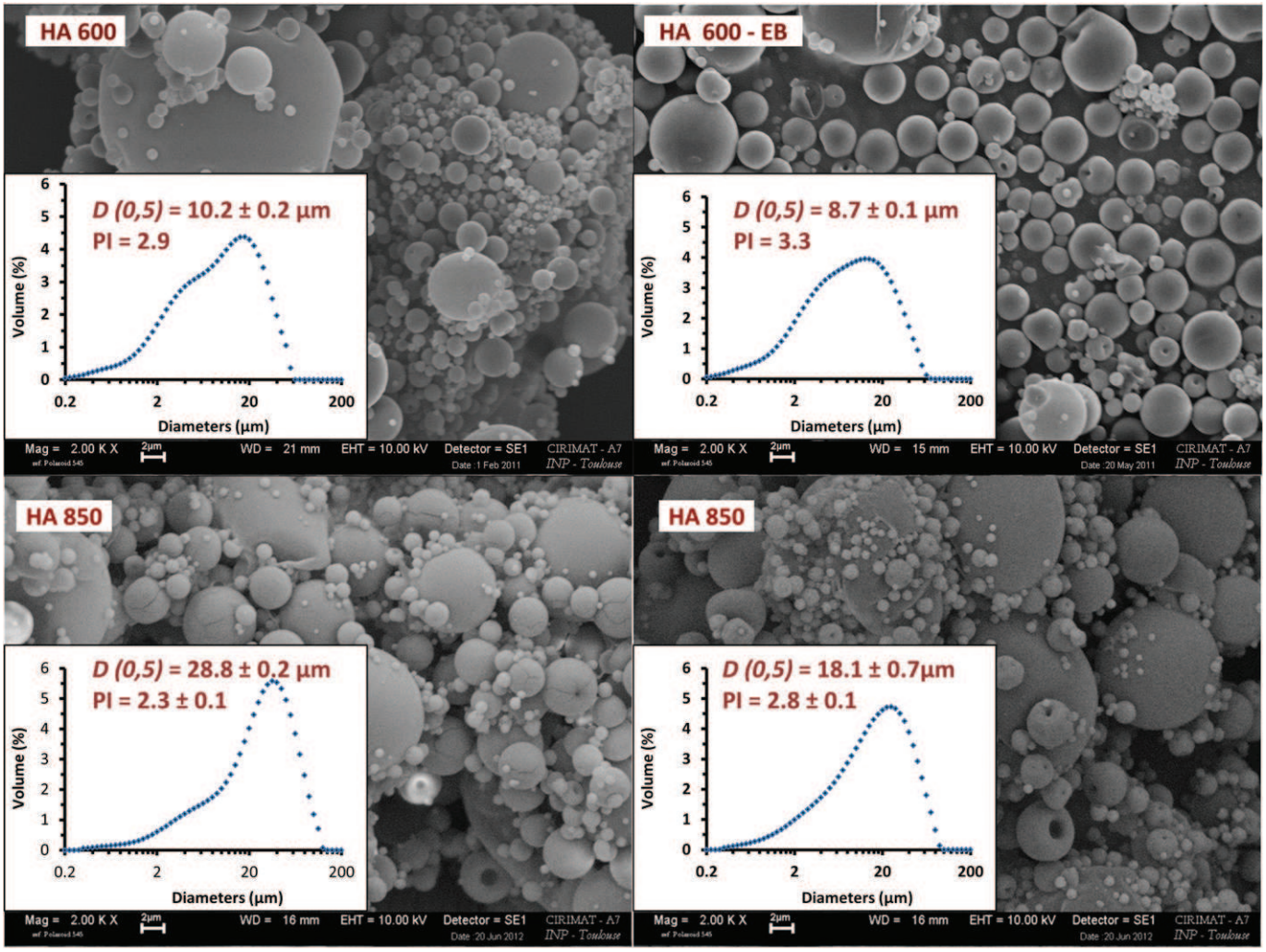

Fig. 6. SEM micrographs and granulometric distributions of HA and HA-EB microspheres (magnification ×2000).

Higuchi model fitted well EB delivery from reference cement, with a coefficient of determination of 0.999. This is not surprising as Higuchi model is currently used to interpret drug release profiles from calcium phosphate cements (see Ref. [14] for review). Mixed calcium phosphate and calcium carbonate cements are highly porous materials due to the free spaces between precipitated crystals, with pore size in the nano/micrometric range [34]. The reference mineral cement, initially constituted of platelets of brushite (B) and lentils of vaterite (V), is shown on Fig. 9C. In vivo, these cements resorption rate is higher than that of usual calcium phosphate cements because of the higher solubility of the $CaCO_3$ metastable phase, vaterite, remaining in the cement final composition [26]. However, since their rate of degradation can be considered much lower than the rate of drug liberation, these mineral cements can be ascribed to the category of nonswellable monolithic systems. As a consequence, drug release is mainly controlled by drug diffusion through mineral matrix in agreement with the Higuchi model.

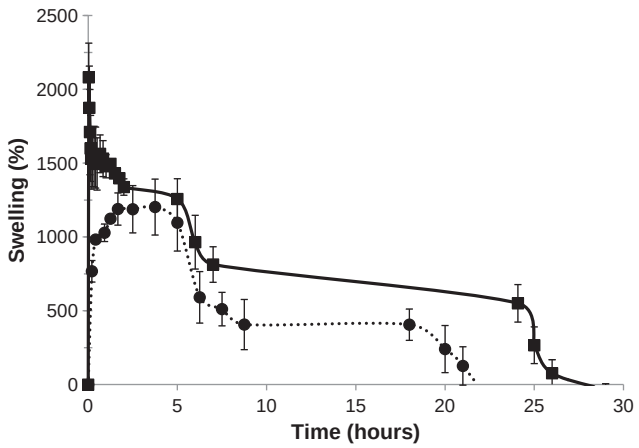

Fig. 7. HA microspheres stability in Tris buffer 0.1 M pH 7.4 as a function of time and HA average molecular weight (●, dotted line: HA600; ■, full line: HA850). Error bars represent the standard deviation for three measurements.

Higuchi model did not fit well with HA-EB and MC-HA-EB curves, except on the first hours of the experiment. In order to better understand the release mechanisms, the Weibull model was applied. This empirical model can be used to describe release diffusion mechanisms during the drug transport through microparticles [29]. Simple interpretations of the exponent b and the timescale t_{scale} values give indications on the possible drug release mechanism. A pure Fick diffusion mechanism corresponds to $b = 1$. Here, all the curves were fitted with functions using $b < 1$. The release mechanisms might thus be ascribed to diffusion in disordered media (with irregular porosity leading to variations in the diffusion coefficient) [35] and/or to diffusion associated to other phenomena like erosion of the matrix [36].

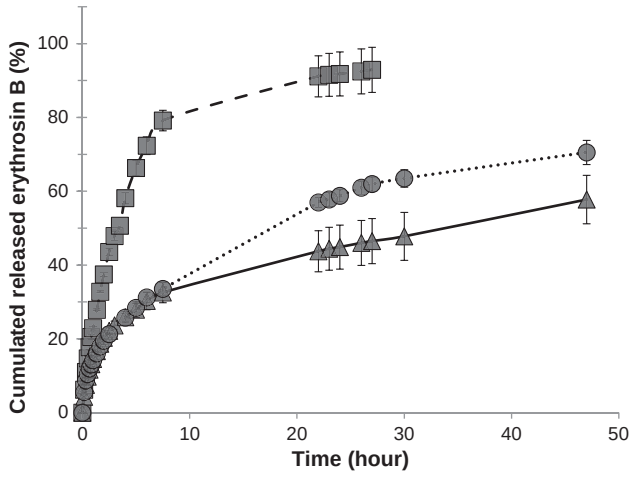

Fig. 8. Cumulative in vitro EB release in Tris buffer pH 7.4 at 37 °C from HA850 microspheres (HA-EB: ■, dotted line), HA850 microspheres loaded cement (MC-HA-EB: ▲, full line) and reference mineral cement (MC-EB: ●, dotted line). Error bars represent the standard deviation for three measurements; lines are obtained by fitting the experimental data points.

In case of HA-EB microspheres, the release kinetics was fast (small t_{scale} and t_{lag} values). This is the direct consequence of the diffusion of the drug through HA particles and gel before complete destructuration. Because hyaluronic acid has carboxyl and hydroxyl groups which can bond with water, the hydrophilic surface is expected to reduce the contact angle, and lead to an increased wettability of the encapsulated molecule, resulting in an improved dissolution [6,5]. A coefficient of determination of 0.998 was also obtained by plotting the linear form of the third semi-empirical equation (dissolutive release mechanism), clearly showing that EB release from microspheres alone is mainly controlled by HA matrix destructuration upon rehydration.

When HA microparticles and mineral cement were associated (MC-HA-EB), EB release appeared to slow down after the first 7.5 hours (high t_{scale} value). The profile presented a t_{lag} and t_{scale} value in the range of 0.14 and 11.59 hours respectively. However, the coefficient of determination of the Weibull modelization was only 0.995, clearly showing that EB release from MC-HA was complex and probably the combination of several phenomena occurring successively. The release profile can be considered in two stages. On the first 7.5 hours, the part of EB released by the HA gel during cement preparation, setting and hardening diffuses freely out of the cement, rending MC-EB and MC-HA-EB release profiles very similar. But during the following hours, EB release rate was significantly slowed in the case of the composite cement. This could be explained by HA microspheres behavior upon rehydration. When hydrophilic polymer based microspheres, such as hyaluronan, are immersed in an aqueous medium, they swell and form a gel diffusion layer that hampers the outward transport of the drug within the matrix, hence producing a controlled release effect [37]. We already observed a similar phenomenon with pectin microspheres–calcium phosphate composite cement [18]. Upon rehydration, HA microspheres become a loose gel which is quite difficult to preserve upon drying for MEB observation. For this reason, HA presence in composite can only be detected as strands mapping mineral particles, these strands being located in specific areas corresponding to initial microspheres location. At a magnification of ×500, "prints" of HA microspheres can be seen within the mineral cement (Fig. 9A, indicated by dotted circles). HA strands, at the bottom of microsphere prints, can be evidenced at higher magnification (Fig. 9B). HA presence within the mineral matrix pores, invading spaces between brushite platelets and vaterite lentils particles, could explain the slowed erythrosin B release from the composite cement, when compared to reference cement.

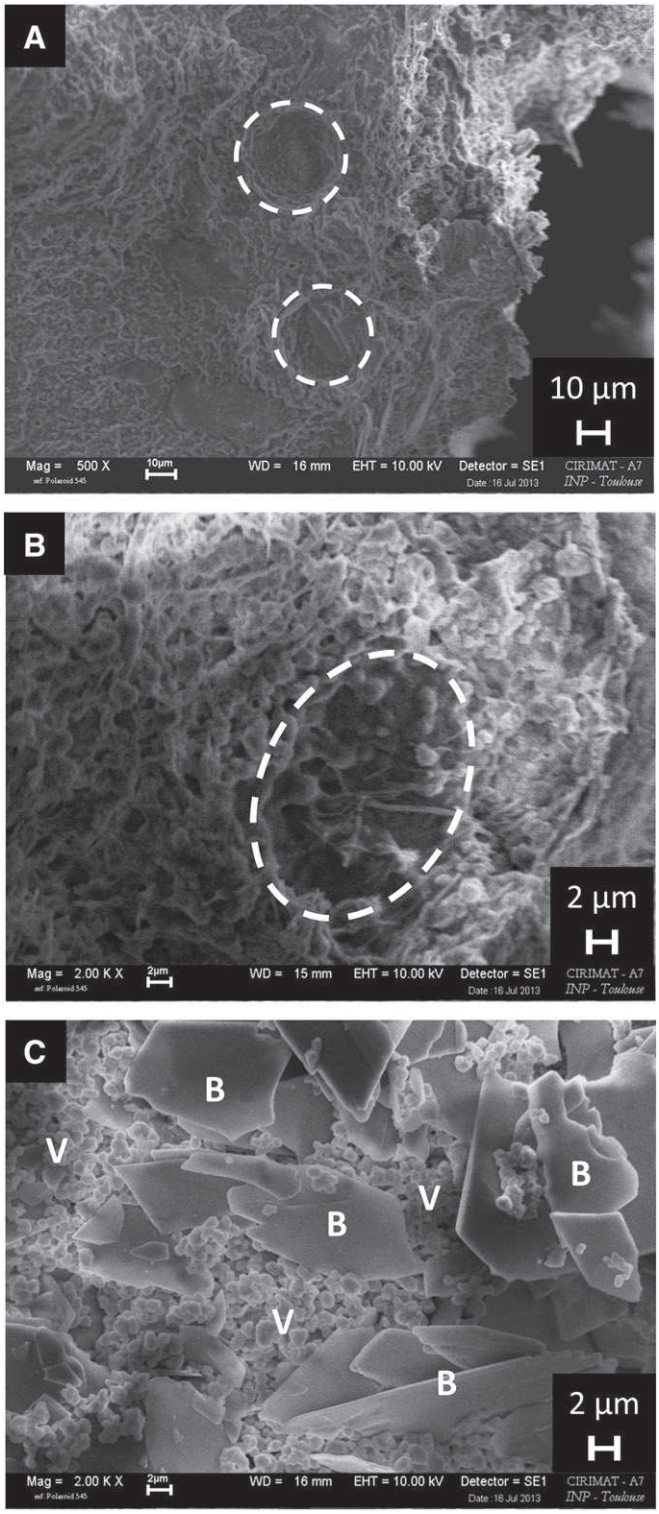

Fig. 9. SEM micrographs of: A: HA850 microspheres loaded cement (MC-HA-EB; magnification ×500); B: HA850 microspheres loaded cement (MC-HA-EB; magnification ×2000); C: reference mineral cement (MC-EB; magnification ×2000). In A and B micrographs, the presence of hyaluronic acid within the mineral matrix is indicated by dotted circles. In C micrograph, platelets of brushite and lentils of vaterite are identified by a B and a V letter, respectively.

4. Conclusion

As a conclusion, the feasibility of introducing HA microspheres in a mineral bone cement, in order to modify its release properties, was demonstrated. Spray-drying permitted a one-pot synthesis, avoiding

time-consuming steps and the use of harsh solvents. The process, compatible with on-line continuous production and easily scaled up, has been optimized to obtain reproducible microparticles with size distributions adapted for the formulation of an injectable bone cement. HA molecular weight and concentration appeared to have a significant influence on process parameters and resulting microspheres. HA850 microspheres degraded in 30 hours when immersed in a buffer medium. However, the introduction of HA microspheres in a mineral cement led to a sustained release, due to HA gel formation within the pores of the mineral matrix which decreases the diffusion rate. Hyaluronic acid microspheres could be of particular interest to formulate bone cements with extended ability to release active compounds.

Acknowledgements

The authors thank the Agence Nationale de la Recherche (ANR — TecSan 2009 program) for supporting this research work (BIOSINJECT — ANR-09-TECS-004 project).

References

[1] M.N. Collins, C. Birkinshaw, Hyaluronic acid based scaffolds for tissue engineering—a review, Carbohydr. Polym. 92 (2) (2013) 1262–1279.
[2] E. Esposito, E. Menegatti, R. Cortesi, Hyaluronan-based microspheres as tools for drug delivery: a comparative study, Int. J. Pharm. 288 (1) (2005) 35–49.
[3] Y. Huh, H.J. Cho, I.S. Yoon, M.K. Choi, J.S. Kim, E. Oh, et al., Preparation and evaluation of spray-dried hyaluronic acid microspheres for intranasal delivery of fexofenadine hydrochloride, Eur. J. Pharm. Sci. 40 (1) (2010) 9–15.
[4] Y.H. Liao, S.A. Jones, B. Forbes, G.P. Martin, M.B. Brown, Hyaluronan: pharmaceutical characterization and drug delivery, Drug Deliv. 12 (6) (2005) 327–342.
[5] M.G. Piao, J.-H. Kim, J.O. Kim, W.S. Lyoo, M.H. Lee, C.S. Yong, et al., Enhanced oral bioavailability of piroxicam in rats by hyaluronate microspheres, Drug Dev. Ind. Pharm. 33 (4) (2007) 485–491.
[6] J.S. Woo, M.G. Piao, D.X. Li, D.-S. Ryu, J.Y. Choi, J.-A. Kim, et al., Development of cyclosporin A-loaded hyaluronic microsphere with enhanced oral bioavailability, Int. J. Pharm. 345 (1–2) (2007) 134–141.
[7] M. Aslan, ÅžimÅŸek Gk, E. Dayi, The effect of hyaluronic acid-supplemented bone graft in bone healing: experimental study in rabbits, J. Biomater. Appl. 20 (3) (2006) 209–220.
[8] X. Xu, A.K. Jha, D.A. Harrington, M.C. Farach-Carson, X.Q. Jia, Hyaluronic acid-based hydrogels: from a natural polysaccharide to complex networks, Soft Matter 8 (12) (2012) 3280–3294.
[9] M. Nageeb, S.R. Nouh, K. Bergman, N.B. Nagy, D. Khamis, M. Kisiel, et al., Bone Engineering by Biomimetic Injectable Hydrogel, Mol. Cryst. Liq. Cryst. 555 (2012) 177–188.
[10] Y. Shona Pek, M. Kurisawa, S. Gao, J.E. Chung, J.Y. Ying, The development of a nanocrystalline apatite reinforced crosslinked hyaluronic acid–tyramine composite as an injectable bone cement, Biomaterials 30 (5) (2009) 822–828.
[11] S. Ahmadzadeh-Asl, S. Hesaraki, A. Zamanian, Preparation and characterisation of calcium phosphate–hyaluronic acid nanocomposite bone cement, Adv. Appl. Ceram. 110 (6) (2011) 340–345.
[12] D. Kai, D. Li, X. Zhu, L. Zhang, H. Fan, X. Zhang, Addition of sodium hyaluronate and the effect on performance of the injectable calcium phosphate cement, J. Mater. Sci. Mater. Med. 20 (8) (2009) 1595–1602.
[13] M.-P. Ginebra, T. Traykova, J.A. Planell, Calcium phosphate cements: competitive drug carriers for the musculoskeletal system? Biomaterials 27 (10) (2006) 2171–2177.
[14] M.-P. Ginebra, C. Canal, M. Espanol, D. Pastorino, E.B. Montufar, Calcium phosphate cements as drug delivery materials, Adv. Drug Deliv. Rev. 64 (12) (2012) 1090–1110.
[15] P.Q. Ruhe, O.C. Boerman, F.G.M. Russel, P.H.M. Spauwen, A.G. Mikos, J.A. Jansen, Controlled release of rhBMP-2 loaded poly(DL-lactic-co-glycolic acid)/calcium phosphate cement composites in vivo, J. Control. Release 106 (1–2) (2005) 162–171.
[16] J. Schnieders, U. Gbureck, R. Thull, T. Kissel, Controlled release of gentamicin from calcium phosphate–poly(lactic acid-co-glycolic acid) composite bone cement, Biomaterials 27 (23) (2006) 4239–4249.
[17] W.J.E.M. Habraken, L.T. de Jonge, J.G.C. Wolke, L. Yubao, A.G. Mikos, J.A. Jansen, Introduction of gelatin microspheres into an injectable calcium phosphate cement, J. Biomed. Mater. Res. A 87A (3) (2008) 643–655.
[18] S. Girod Fullana, H. Ternet, M. Freche, J.L. Lacout, F. Rodriguez, Controlled release properties and final macroporosity of a pectin microspheres–calcium phosphate composite bone cement, Acta Biomater. 6 (6) (2010) 2294–2300.
[19] J.R. Popp, K.E. Laflin, B.J. Love, A.S. Goldstein, Fabrication and characterization of poly(lactic-co-glycolic acid) microsphere/amorphous calcium phosphate scaffolds, J. Tissue Eng. Regen. Med. 6 (1) (2012) 12–20.
[20] H. Liao, X.F. Walboomers, W.J.E.M. Habraken, Z. Zhang, Y. Li, D.W. Grijpma, et al., Injectable calcium phosphate cement with PLGA, gelatin and PTMC microspheres in a rabbit femoral defect, Acta Biomater. 7 (4) (2011) 1752–1759.
[21] K.H. Khayat, Viscosity-enhancing admixtures for cement-based materials — an overview, Cem. Concr. Compos. 20 (2–3) (1998) 171–188.
[22] M. Bohner, U. Gbureck, J.E. Barralet, Technological issues for the development of more efficient calcium phosphate bone cements: a critical assessment, Biomaterials 26 (33) (2005) 6423–6429.
[23] M.H. Alkhraisat, C. Rueda, F.T. Mario, J. Torres, L.B. Jerez, U. Gbureck, et al., The effect of hyaluronic acid on brushite cement cohesion, Acta Biomater. 5 (8) (2009) 3150–3156.
[24] R. Vehring, Pharmaceutical particle engineering via spray-drying, Pharm. Res. 25 (5) (2008) 999–1021.
[25] In: K. Masters (Ed.), Spray-Drying, Wiley, Handbook New York, 1990.
[26] C. Combes, R. Bareille, C. Rey, Calcium carbonate–calcium phosphate mixed cement compositions for bone reconstruction, J. Biomed. Mater. Res. A 79A (2) (2006) 318–328.
[27] In: Europe Co (Ed.), European Pharmacopoeia 7th ed., 2011, (Strasbourg, France).
[28] T. Higuchi, Mechanism of sustained-action medication. Theoretical analysis of rate of release of solid drugs dispersed in solid matrices, J. Pharm. Sci. 52 (1963) 1145–1149.
[29] V. Papadopoulou, K. Kosmidis, M. Vlachou, P. Macheras, On the use of Weibull function for the discernment of drug release mechanisms, Int. J. Pharm. 309 (2006) 44–50.
[30] C. Nastruzzi, E. Esposito, R. Gambari, E. Menegatti, Kinetics of bromocriptine release from microspheres: comparative analysis between different in vitro models, J. Microencapsul. 11 (5) (1993) 565–574.
[31] W. Liu, W.D. Wu, C. Selomulya, X.D. Chen, Uniform chitosan microparticles prepared by a novel spray-drying technique, Int. J. Chem. Eng. 2011 (2011) 1–7.
[32] A.B.D. Nandiyanto, K. Okuyama, Progress in developing spray-drying methods for the production of controlled morphology particles, Adv. Powder Technol. 22 (2011) 1–19.
[33] M.A. Ré, L.S. Messias, H. Schettini, The influence of the liquid properties and the atomizing conditions on the physical characteristics of the spray-dried ferrous sulfate microparticles, Drying B (2004) 1174–1181.
[34] M. Espanol, R.A. Perez, E.B. Montufar, C. Marichal, A. Sacco, M.P. Ginebra, Intrinsic porosity of calcium phosphate cements and its significance for drug delivery and tissue engineering applications, Acta Biomater. 5 (7) (2009) 2752–2762.
[35] In: P. Macheras, A. Iliadis (Eds.), Modeling in Biopharmaceutics, Pharmacokinetics, and Pharmacodyanmics, Springer, New-York, 2006.
[36] D.Y. Arifin, L.Y. Lee, C.-H. Wang, Mathematical modeling and simulation of drug release from microspheres: implications to drug delivery systems, Adv. Drug Deliv. Rev. 58 (12–13) (2006) 1274–1325.
[37] S.T. Lim, G.P. Martin, D.J. Berry, M.B. Brown, Preparation and evaluation of the in vitro drug release properties and mucoadhesion of novel microspheres of hyaluronic acid and chitosan, J. Control. Release 66 (2–3) (2000) 281–292.